



Non invasive contact electrodes for *in vivo* localized cutaneous electropulsation and associated drug and nucleic acid delivery

Serge Mazères^a, Davorka Sel^b, Muriel Golzio^a, Gorazd Pucihar^b, Youssef Tamzali^c, Damijan Miklavcic^b, Justin Teissié^{a,*}

^a IPBS CNRS Université de Toulouse (UMR 5089), 205 route de Narbonne, 31077 Toulouse, France

^b Faculty of Electrical Engineering, University of Ljubljana, Trzaska c. 25, 1000 Ljubljana, Slovenia

^c Clinique équine, Ecole nationale vétérinaire, Toulouse, France

ARTICLE INFO

Article history:

Received 22 August 2008

Accepted 2 November 2008

Available online 19 November 2008

Keywords:

Electropulsation

Electrodes

Electrochemotherapy

Electrogenotherapy

Electroporation

ABSTRACT

For an effective tissue controlled electropermeabilization as requested for electrochemotherapy and electrogenotherapy, it is very important to have informations about the electric field distribution provided by a defined set of electrodes. Computer simulations using the finite element models approach predicted the associated field distributions and currents. Phantoms made of gels with well-defined electrical conductance were used to measure the current responses of a new electrode geometry (wires). A good agreement between the measured and predicted currents was observed supporting the validity of the prediction for the field distribution.

Field distribution was observed to be very localized and highly homogeneous with the new concept of contact wire electrodes. They allowed to focus the field effect along the surface of the tissue to induce a controlled release of drugs or plasmids. Non invasive (contact) electrodes can be moved rapidly on the body and avoid puncturing the skin and the tissue. They can be used for large surface effects, to treat the skin and subcutaneous tumors. The use of contact electrodes after drug or DNA intradermal injection were validated by clinical treatment of large surface skin tumors and by *in vivo* imaging of permeabilization or of gene expression.

© 2008 Elsevier B.V. All rights reserved.

1. Introduction

Cell treatment with high intensity electric field pulses provokes a change in the membrane structure leading to a loss of its barrier function, a phenomenon called electropermeabilization or “electroporation” [11,23]. By a proper choice of the parameters of the applied electric field (i.e. amplitude, pulse duration and number of pulses), this change in the membrane permeability can be reversible preserving cell viability or irreversible leading to cell death. Electropermeabilization brought the technical possibility to introduce (load) exogenous compounds (drugs, plasmids) into cells. It is now used as a very efficient way for drug, oligonucleotide, antibody and plasmid delivery *in vitro* and *in vivo* for clinical applications [11,23].

Electrotransfer of plasmids has been performed *in vivo* on several tissue types including skin, liver, tumor, muscle, brain, testis and spleen [2,5,15,18,24,29,34]. Many studies have now shown that plasmid electrotransfer can lead to a long-lasting therapeutic effect in various pathologies, such as cancer, blood disease, or muscle ischemia. These have been reviewed in [3,6,14,20]. Clinical develop-

ments are obtained under optimized electrical conditions [35]. The local field strength appears as the critical parameter for *in vivo* studies [8,12,28]. Its value must be larger than a threshold to trigger the permeabilization process but below a value inducing irreversible damages. These biological effects are under control of the pulse duration. Therefore application of square wave pulses appears the most suitable. Field effects on cells in tissue are rather similar from what is obtained for cells in suspension. They nevertheless depend on the cell density [25] and on the different shapes of cells [36]. The local field strength remains the critical parameter [35]. It is the field distribution in the tissue which is important [1,21,20].

While field distribution is homogeneous when diluted cells are pulsed in suspension between parallel plate electrodes, the problem is much more complex in tissue. As the field results from a voltage applied between two electrodes, the electrode configuration is clearly controlling the field distribution and therefore the effective uptake. Various electrode configurations for therapeutic purposes are available such as parallel plates, wire and contact plate electrodes [9] as well as needle electrodes and needle arrays [13,19,27,37].

Electrode configuration influences the electric field distribution in tissue. Needles are popular but mechanically invasive and the associated field distribution is very heterogeneous [4,17,22]. They were shown to induce local burning due to their very high current

* Corresponding author.

E-mail address: justin.teissie@ipbs.fr (J. Teissié).

density close to the electrode surface. Joule heating can therefore be very high [26]. Parallel plates are rather popular when their use is possible as when pulsing mouse thigh muscle [7] or when skin pinching is possible [5,29]. Meander electrodes affect the stratum corneum (SC) and support transdermal delivery [17].

It is therefore necessary to choose appropriate electrode configuration for the particular target tissue before it is exposed to therapy. In order to obtain such information, electric field distribution in tissue has to be computed in advance by means of modeling. Due to tissue complexity, analytical solution of such problem is almost impossible. Therefore in most cases numerical modeling techniques are used. Mostly finite element method and finite difference methods are applied [31]. Both numerical methods have been successfully used and also validated by comparison of computed measured electric field distribution and associated consequences in tissues [32]. Finite element model validation by computed reaction current was used only very recently [32]. Current measurement is much faster than imaging method, which can be used to obtain electric field distribution in tissue. Therefore we selected the finite element model validation with experimental current measurements as a fast method of model validation.

But it is also well known that numerical methods are computationally demanding. Therefore, it is required to search for simplifications in modeling process which can decrease computational efforts and at the same time preserve the accuracy of the result, i.e. electric field distribution or current. Such simplifications can be performed either on the description of electrodes or on the physical properties of tissue. In this work, we have assumed simple shapes for electrodes (polygonal rather than cylindrical). Tissues (in our case: dermis and epidermis, the SC being bypassed within a few microseconds after the pulse onset) were assumed to have a homogeneous conductivity and soft gels prepared in saline buffers can be used as phantoms. This is indeed in fair agreement with *ex vivo* direct observations where large domains with homogeneous conductance are present in tumors [39].

Subcutaneous electropulsation is known to be relevant of clinical applications (subcutaneous tumors) and for gene therapy (DNA vaccines). It was predicted that contact wire electrodes should provide targeting of the field effect under the skin. Contact wire electrodes have been shown to be very convenient when large tissue surfaces (several square centimeters) must be treated due to the ease of their use [16,30]. The field distribution from the simulation was validated by comparing the current values given by the simulation and their experimentally measured value (Fig. 1). Field lines were definitively proved to be focused along the skin. These physical predictions and conclusions were checked *in vivo*. As a conclusion, contact wire electrodes offer an approach, where electropulsation *in*

vivo can be efficiently, easily and safely performed at the cutaneous level.

2. Materials and methods

2.1. Tissue phantom

The cutaneous tissue is an ohmic conductor as soon as the stratum corneum is electropermeabilized and as long as the tissue is not destroyed by the field. Tissue phantom was made of gelatin (2.4% w/v) in phosphate buffer (concentration 20 mM, pH=7.4) and NaCl (concentration 150 mM), with electrical parameters and characteristics close to real tissue. This is actually a gel with some rigidity when cooled. Due to moisture of the gel a good electrical contact was attained with electrodes in direct contact with the gel. Fresh gel was prepared from a buffer before each experiment and its conductivity was measured (conductimeter Hanna HI8820N, Germany). Tissue phantom conductivity was 1.5 S/m.

The phantom tissue was prepared in a Petri dish of 35-mm diameter. The thickness of the gel was adjustable to 2, 4 or 6 mm, depending on the requirements of the specific experiment. The thickness of gel was controlled by pouring a given volume of the hot liquid gel in the dish.

The voltage pulse was obtained with a high voltage square wave pulse generator (CNRS Jouan PS 10, France) (Fig. 1). Voltage up to 1000 V can be delivered as long as the current was less than 8 A. On this system, if a current surge exceeds this limiting value (8 A), an automatic switch is triggered for safety reasons and the pulse is discontinued. A resistor R was inserted in series with the electrode array to be used to monitor the current. Both a fraction of the voltage pulse delivered by the generator and the voltage across the resistor R were digitized (8-bits resolution) and stored on line with a transient recorder (Data Lab DL 905, UK). The stored signals were observed on an oscilloscope or analyzed on a MacIntosh LCIII microcomputer (Apple, USA) by using an ADA4 interface with an Excel subroutine. The system was calibrated for the current by using an ohmic calibrated high power resistor in place of the electrode-gel set up. Applied voltage was in the range 100 V to 500 V, in increments of 100 V. The pulse length was 0.1 ms (to limit Joule heating). By plotting U/I ratio during the pulse application, material conductivity was observed to be constant. A linear response of the system was observed for increasing values of the applied voltage (up to 1000 V). In some experiments, lower applied voltages (0 to 100 V) were studied with increments of 25 V. (Fig. 1)

Reproducibility of replicates accuracy in each experiment was high. It was the reason to assume three replicates per experiment were sufficient. Based on the fact that replicate results in all experiments were very similar we can assume that random measurement error was negligible.

2.2. Electrodes

Contact wires were two parallel stainless steel rods with a diameter of 1 mm, a length from 10 to 20-mm at a distance ranging from 4- to 9-mm for the different models (Figs. 2–5). Their penetration in the gel (or the extent of their contact with the skin) can be adjusted by exerting different pressures. A conductive gel was used to improve the contact with the skin in the *in vivo* experiments [39].

2.3. Simulation: finite element method

A three-dimensional finite element model of a gel in Petri dish with contact electrodes was designed using software package Emas produced by ANSOFT Corporation.

The geometry under study was moderately complex, involving few physical objects (gel, electrodes) with specific geometrical and

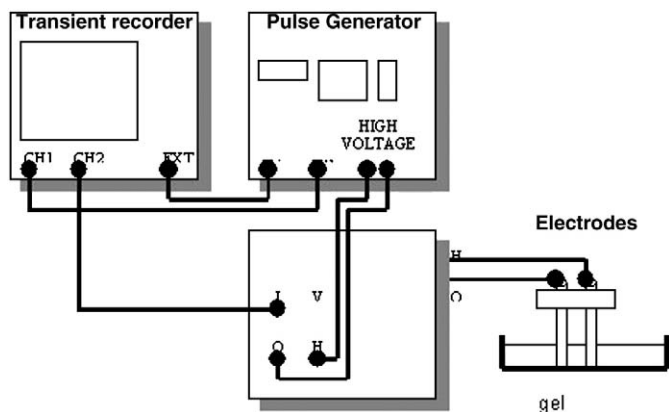


Fig. 1. Electrical set up. The high voltage is applied between the two electrodes in contact with the gel. The voltage and the current are recorded on line, digitized and stored. The time course of their ratio gives access to the time change of the impedance of the gel during the pulse.

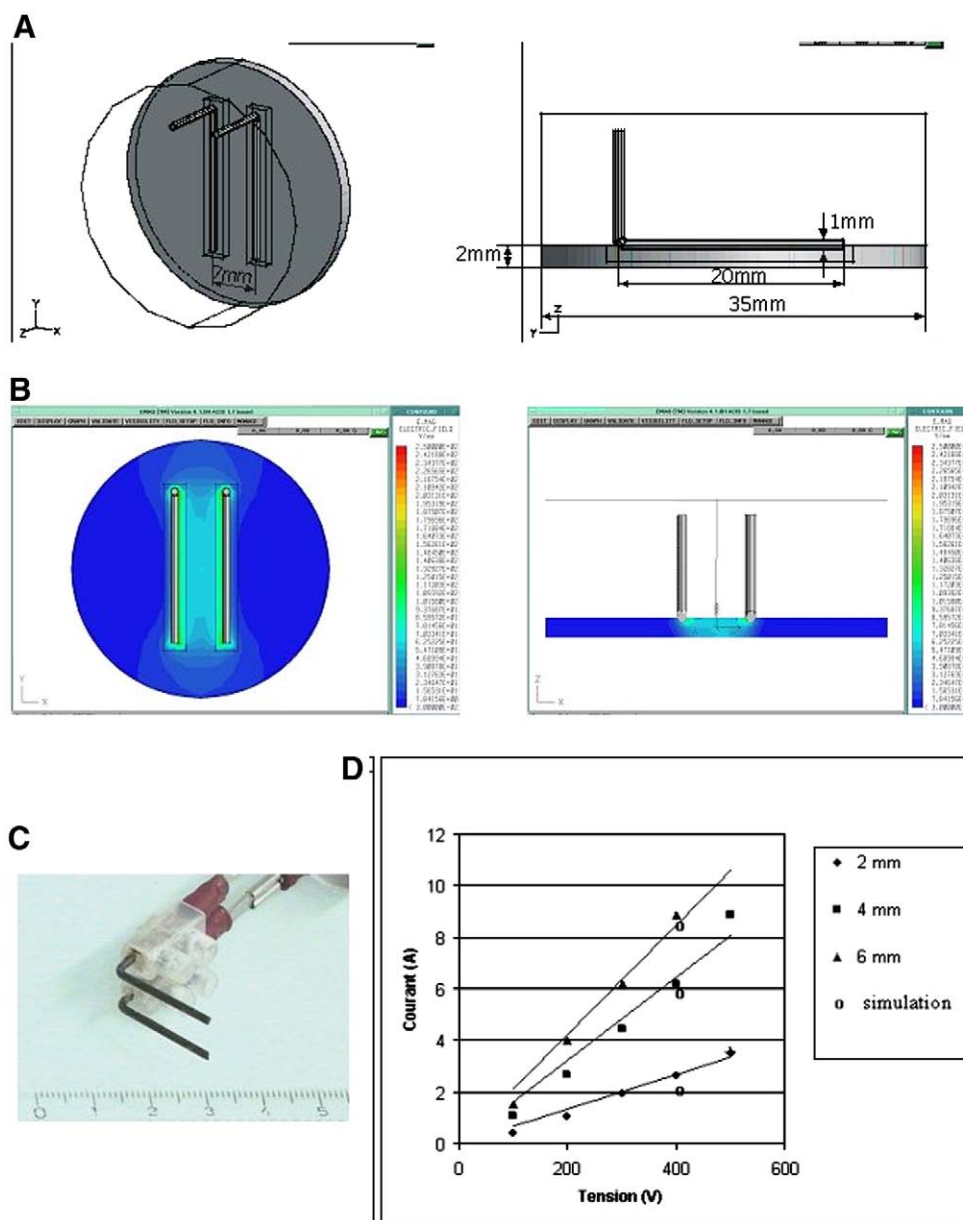


Fig. 2. Simulations and experiments with contact wire electrodes. A— drawing of the electrodes. B— field simulation: side and top views. Colour coding was used with the scale on the right. Red means high local field and blue a low value. This is under the control of the applied voltage on the electrodes. C— picture of the electrodes. The width between the two wires is set at 9 mm. Their length is 20 mm. This is the model which is used for the simulation shown in B. D— current–voltage plot. They were obtained by using the procedure shown in Fig. 1. A 100 μ s controlled voltage pulse was applied on the electrodes in contact with the gel. Different gel thicknesses were used. The continuous lines were the simulation predictions assuming an ohmic behaviour. (For interpretation of the references to colour in this figure legend, the reader is referred to the web version of this article.)

material properties. To simplify modeling and solution process the basis of finite element approach is to divide the volume into many finite elements, each with much simpler properties. In software package EMAS, when automatic mesh generation is selected, these elements have the shape of tetrahedrons. Material properties within each element are uniform.

Our experimental model was described with equations for steady electric current in volume conductor, due to the fact that constant voltage was applied to homogenous and isotropic conductive materials, i.e. gel. Steady electric current in volume conductor was described by means of Laplace equation. Solution of Laplace equation requires two types of boundary conditions, which are Dirichlet boundary condition and Neumann boundary condition. The former was defined as scalar normal electric potential on the surface of electrodes (constant voltage) and the latter as the first derivative of the scalar potential. In software package Emas v.4 Neumann boundary

condition is automatically set to zero due to the fact that the model is surrounded by an ideal insulator.

Mesh was denser in regions around electrodes than at the edge of the Petri dish. The reason for such meshing was the significantly smaller dimensions of electrodes, than those of the surrounding gel. Current densities were higher close to the electrodes. 8-faceted electrodes were used [32]. In first experiments, they were immersed by 0.5-mm in gel and in second experiments by only 0.25-mm.

2.4. *In vivo* dye or DNA delivery

All experiments on mice were performed in agreement with the recommendations of the ethical committee of the CNRS.

Fur was removed with a depilatory lotion (Veet, France) two days before experiments. Animals were kept under isoflurane/air anesthesia during the whole procedure. A predetermined amount plasmid

DNA (coding for a Ds Red2 fluorescent protein under a CMV promoter) in PBS solution (0.5 µg/µl of plasmid) was injected ID under the skin. The volume of DNA, kept constant at 20 µl in mice, was injected with a Hamilton syringe through a 26G needle (Hamilton, Bonaduz, Switzerland). Electrotreatments were applied by bringing the electrodes ($d=6$ mm) directly in contact with the skin of the animal back apart at the injection site. Contact between the electrodes and the skin was assured by a conductive gel and maintained by gently pressing electrodes against the skin during pulse delivery. A 60 mm² skin surface was submitted to the field. The electric field was applied as a train of repetitive square wave pulses. A voltage ranging between 60 and 240 V was applied along eight 20 ms square wave pulses with polarity inversion between each pulse at 1 Hz.

2.5. *In vivo* fluorescence optical imaging

Visualization of fluorescent protein expression is obtained with a fluorescence stereoscope (Leica Model LZIII) equipped with a cooled CCD camera (Roper coolsnap fx). A conventional light source (Arc mercury lamp) and the filter set give the proper illumination [43]. Expression was followed on the same animal over several weeks after electrical gene transfer. Animals were kept anaesthetized during the imaging procedure. They were simply brought on the microscope stage and the back of the animal was observed.

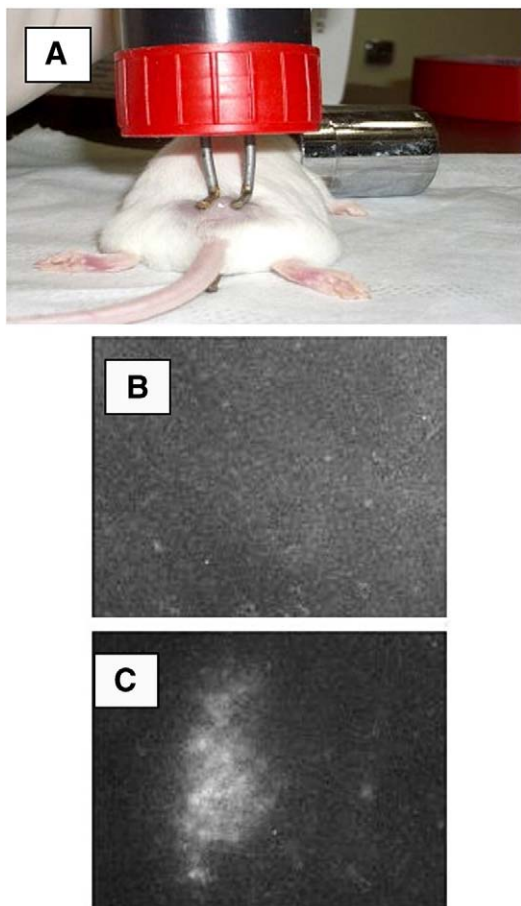


Fig. 3. Electrotherapy of the skin with contact wire electrodes. A Ds red coding plasmid was intradermally injected. The electrodes (electrode distance 4 mm) were brought on the sides of the injection point (A). 5 pulses of 20 ms with a voltage to electrode distance of 200 V/cm were applied at a frequency of 1 Hz. Skin was observed by local whole body fluorescence imaging 72 h after the electrical treatment. The top view (B) is with injection of 100 µg of plasmid and the bottom view (C) is with injection of 100 µg of plasmid followed by electropulsation. Expression (red fluorescence emission) is detected in the part of the skin which was between the electrodes (white part of the B/W picture).

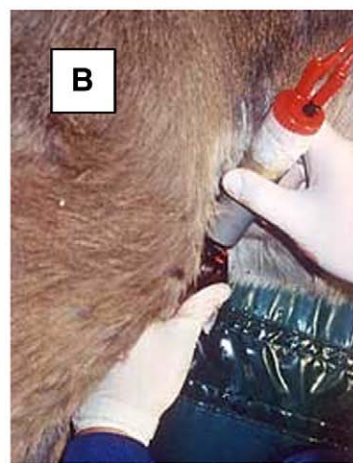


Fig. 4. Sarcoids ECT. A— a general view of the clinical treatment. The horse is lying on its back under general anesthesia. This is controlled by the assistants on the left side. The vet surgeon is treating the tumors between the back legs by bringing the electrodes in contact with the shaved skin. The drug (or the plasmid) was previously IT injected. B— a detailed view of the contact wire electrodes during the horse treatment. Moving the electrodes along the sarcoid surface and changing their orientation to obtain crossed field directions is easily obtained to get an optimized electrical treatment of the skin tumor.

2.6. Sarcoids electrochemiotherapy

Clinical trials were operated at the equine clinic (ENVT). Owners consent was obtained after description of the clinical trial. All animals were treated under short term general anesthesia with intravenous agents. The tumor site was surgically prepared.

Cisplatin (Sigma-Aldrich St-Quentin-Fallavier, France) was dissolved in phosphate buffer saline to obtain 1 mg/ml solutions. It was then administered with insulin syringes by injections (0.2–0.3 ml 6 mm apart in the 3 dimensions) into the tumor mass and 1 cm of apparently healthy margin to reach a concentration of approximately 1 mg/cm³ of target tissue). Tumor volume V (cm³) was estimated by measuring the 3 greater diameters (a, b and c in cm) with a Vernier caliper and application of the formula: $V=abc \times \pi/6$.

Within 5 min after cisplatin IT injection, the electrodes (electrode distance 9 mm, pulsed surface 90 mm²) were put into direct contact with the skin on the tumor surface and the margins. The contact was ensured by application of a conducting gel. Two runs of 8 electric pulses (duration 100 µs with 1300 V to cm voltage to distance ratio which corresponded to a voltage of 1170 V) were delivered at a frequency of 1 Hz in two orthogonal directions per site (just by turning by 90° the electrodes orientation) [33]. When the tumor diameter exceeded 9 mm the procedure was repeated by replacing the

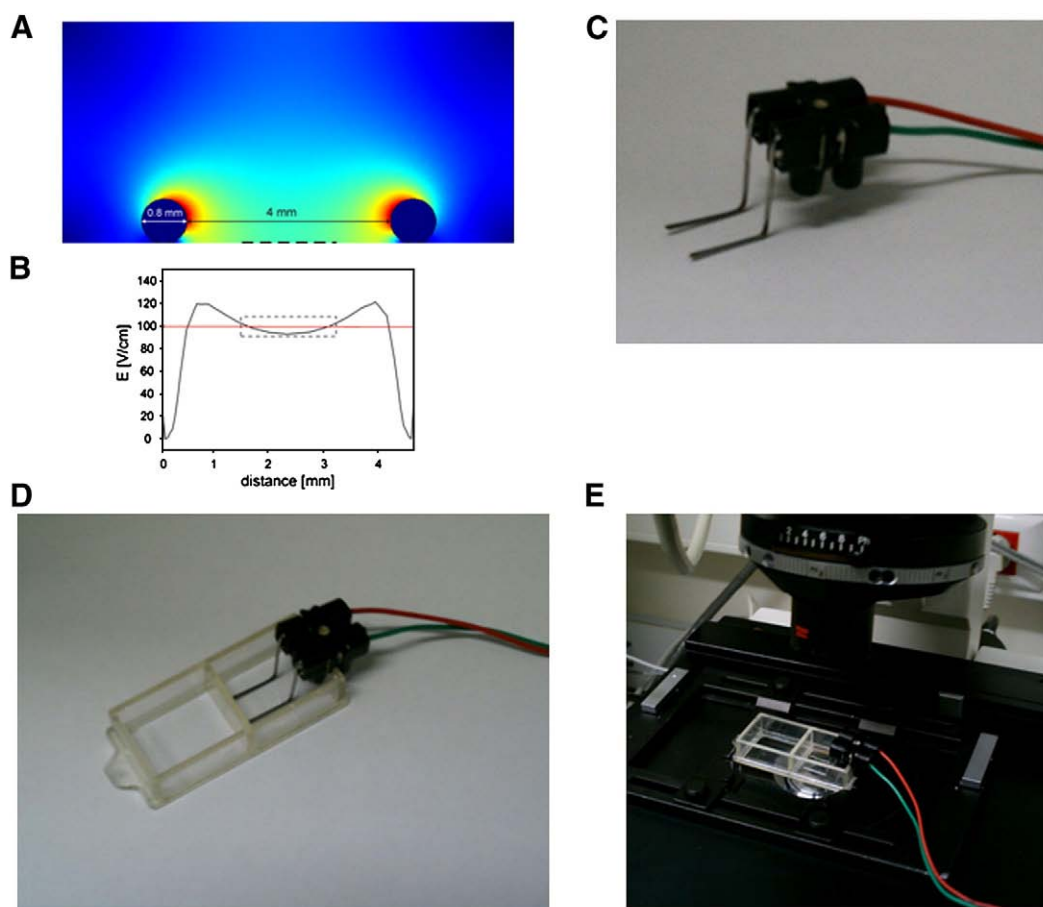


Fig. 5. Computation of electric field distribution between the electrodes in the *in vitro* configuration. A—Electrodes with a 0.8 mm diameter were at a 4 mm distance and positioned to the bottom of the dish. The extracellular medium conductivity was set to 1.4 mS/cm. The dashed lines delineate the surface where a homogeneous field is present. B— Graph of the electric field distribution. The horizontal line denotes the voltage to distance ratio (U/d). The dashed square is the volume where a homogeneous field was present (less than 10% variation). C— Electrode set up. The wires are connected to the pulse generator. D— Electrodes on a dish. In this case, a labtek dish is used. The electrodes are in contact with the bottom of the dish. E— The dish with the electrodes is on the microscope stage.

electrodes on another site in order to cover the entire tumor surface and 1.5 cm of cutaneous margin.

3. Results

3.1. Field distributions

Simulations showed that field 3D distributions were highly inhomogeneous (Fig. 2). High fields were predicted at the contact of the electrodes. However a homogeneous field with a fairly high value was obtained on a thin (about 1 mm thick) layer along the gel surface, all across the electrodes width. The magnitude of the field was decreased when monitored deep in the gel. This means that the current was flowing everywhere in the tissue but that the field was intense specifically along the surface. As a consequence, a targeting of the field effect is obtained at the position expected for a cutaneous treatment. Currents were experimentally measured on the gel system (Fig. 2). An ohmic behaviour was observed meaning that the conductance of the gel was just a scaling parameter. The current at a given voltage was strongly dependent on the gel thickness. A poor agreement was observed only when the thickness of the gel was 2 mm. This observation was already present in our previous investigation with needle electrodes [32]. With the needle array, the observation was previously associated to a surface conductance along the Petri dish surface, which would enhance the current at the bottom of the dish.

The penetration of the electrodes across the gel surface was changed to mimic what is experimentally done when pushing the electrodes against the tissue (skin) in the *in vivo* experiments. The simulation predicted an increase in current with the deeper (0.5 versus 0.25 mm) penetration, i.e. with an increased surface contact (data not shown).

The prediction of a high field close to the electrodes is very positive. It is well known that the stratum corneum must be brought to a conductive state by a large field effect to obtain a cutaneous effect with non invasive contact electrodes. This is facilitated by the present geometry.

3.2. Gene electrotransfer in mice

This geometry of electrodes was checked for its suitability in *in vivo* experiments. Using a train of 8 20 ms pulses, intradermal gene electrotransfer was efficiently obtained. Fluorescent protein expression is observed by stereomicroscopy imaging. This gives access to the mapping of expression. Expression was detected in all parts of the back of the animal between the two electrodes confirming the predicted local homogeneity of the field distribution. Expression was absent in all other parts of the animal back (Fig. 3). A targeting of expression was obtained with the wire electrodes electropulsation with the support of the ID plasmid injection. We applied increasing voltages (to obtain up to 400 V to cm) to optimize the level of expression, which was quantified by the level of fluorescence detected in

the *in vivo* imaging method. An increase in expression was observed with an increase in voltage. But a limit was present. Skin burning was observed at the level of the contact with the electrodes only when large voltages were applied (350 V to cm). This is the direct « biological » consequence of the prediction that higher fields and associated current densities were induced at the close contact of the electrodes. This was in agreement with the prediction and previous observations with needle electrodes [20].

3.3. Equine ECT

Another *in vivo* use of these electrodes is the electrochemotherapy of equine sarcoids [30]. Sarcoids represent more than 50% of cutaneous tumors in equids. There is no universal treatment against sarcoids and surgical treatment leads to frequent relapses. Electrochemotherapy requested the delivery of a high field specifically under the skin where the drug was injected.

Very positive results with the contact wire electrodes were obtained proving the homogeneous permeabilization of the cutaneous tumors bringing the penetration of the cytotoxic compound. Some limits were predicted by the simulation and were experimentally present. We observed that when the electrodes were pushed strongly against the animal skin, bringing an increase in the surface in contact, the current which was delivered by the electropulsator was increased. In fact in many experiments, the current security was triggered when the pressure was too high. This observation is the experimental evidence of the prediction that if the penetration of the electrodes against the surface of the gel was deeper, the current would be larger. But when this contact problem was avoided by a careful handling of the electrodes, sarcoid ECT was very effective [30]. No damage was induced and the treatment can be repeated with a more gentle contact. Objective responses were detected in more than 97% of the treated horses (more than 200 tumors). Complete responses were obtained in 93% with a follow up of more than 7 years in all cases. Tumors were eradicated with success with diameters up to 5 cm. The treatment was easy due to the ergonomics of the system which allowed to cover the whole tumor and its surroundings very easily within a short period (Fig. 4). Indeed a controlled release over a large surface is provided.

3.4. *In vitro* application of wire contact electrodes

Besides the *in vivo* experiments, this electrode design can be useful for *in vitro* experiments. We checked if the “homogeneous localized” field distribution was obtained when bringing the wire electrodes in contact with an insulator and keeping them immersed in a conducting medium. A similar approach for simulation was used as for the phantoms. As shown in Fig. 5, we obtained as expected a homogeneous field in the center of the width between the two electrodes. One limit is that the distance between the two electrodes has to be large when compared to their thickness [38]. A practical application of this set up is when working in a petri dish or on a microscope slide. When the electrodes are in contact with the dish (or the slide), a drop of a cell suspension, forms a bridge between the two electrodes. It will be submitted to a field distribution as pictured in Fig. 5. This is used to pulse cells under a microscope and observe them on line during the pulse or just after it [8,12].

4. Discussion

The general conclusion of this study is that there is a good agreement between simulation and experiments on gel using current as a monitor. This is a further support of the numerical approach which we proposed with needle electrodes. Computer simulations using the finite element models approach predicted well the associated field distributions and currents. We can predict the field

distribution in the tissue for the different electrode geometries. This was used in the present study for an optimization of their designs for a localized release of drugs and plasmids at the skin level.

Limits in our approach are that we made the assumptions that a tissue was a homogeneous electrical body and that its conductance was not changed during the voltage pulse application. These aspects need further studies. But we observed an ohmic behaviour. Therefore our conclusions remain valid at the onset of electropermeabilization under the assumption that the tissue is an association of electrically homogeneous patches (as in the case of treatment of dermis). As far as the homogeneity of the pulsed tissue is concerned, one may be concerned that the skin is present between the electrodes and the target subdermal tissue. But the stratum corneum becomes conductive under electrodelivery conditions giving a homogeneous field within tumors [39].

Indications are clear for the choice of these electrodes for clinical applications. When a surface controlled release is the clinical target as for electrochemotherapy of large cutaneous tumors (sarcoids in horses) contact wire electrodes are the most suitable systems. Due to their ergonomics, they are easy to handle and can be moved on the organ surface to treat successive surfaces and obtain the electro-treatment on a large area (equine sarcoids with several centimeters in diameter were easily treated in equine electrochemotherapy). Only a superficial effect is obtained due to the localized field effect. But, by repeating the clinical treatment, the eradication of thick tumors was obtained [30]. It should be pointed out that at a given voltage to distance ratio, the depth of effective field penetration is increased with a larger width between the electrodes. At given voltage and electrode width, the current is under the control of the electrode length and the tissue contact. The contact wire system, with a limited field penetration depth, is also suitable for gene transfer in the dermis (as shown by our results) where Antigen Presenting Cells are abundant (for experiments on DNA electroimmunization) [5] and for IL12 expression [16]. We recently showed that these electrodes geometry was very effective for DNA immunization for antiangiogenesis concerns [40]. Coupling between ECT and IL12 electrogenotherapy by using these electrodes can therefore be obtained to boost the destruction of tumors as reported on mice models [41,42]. The geometry of these contact wire electrodes can be as simple as we described in this paper. A key feature of the wire contact electrodes is their cylindrical shape. Sharp edges must be avoided as they will induce local high field and current [10]. This means that local burning may then be present. This is the case if rather than using cylindrical wires as described in this report, plate electrodes are used by bringing only their sharp edges in contact with the skin. Another limit with the “plate contact” electrodes (so called meander electrodes) [17] is the ratio of the surfaces of the electrodes and of the skin is larger than with the wire contact electrodes. More sophisticated (and expensive) designs are present on the market such as « meander electrodes » but a precise description of the associated field distribution is lacking [17]. They are designed to obtain an effect specifically on the stratum corneum to obtain a transdermal delivery [44]. Another key feature is that the width must be large relative to the wire diameter to get the homogeneous field distribution along the surface [38].

Clearly due to the flexibility in their use when multiple treatments on the same patient are required, contact non-invasive electrodes offer a lot of convenience.

Acknowledgements

The financial support of the EU cliniporator program and of various grants of the Minister of Sciences, Education and Sport of the republic of Slovenia must be acknowledged. This cooperation was under the Slovenian French Proteus and CNRS PICS programs. Grants of the « ligue contre le cancer », of the region Midi-Pyrénées and of the CNRS CEA “Imagerie du petit animal” program made possible the *in vivo* experiments.

References

- [1] I.G. Abidor, L.H. Li, S.W. Hui, Studies of cell pellets: II. Osmotic properties, electroporation, and related phenomena: membrane interactions, *Biophys. J.* 67 (1994) 427–435.
- [2] H. Aihara, J.I. Miyazaki, Gene transfer into muscle by electroporation *in vivo*, *Nat. Biotechnol.* 16 (1998) 867–870.
- [3] F. Andre, L.M. Mir, DNA electrotransfer: its principles and an updated review of its therapeutic applications, *Gene Ther.* 11 (Suppl 1) (2004) S33–S42.
- [4] S.B. Dev, D. Dhar, W. Krassowska, Electric field of a six-needle array electrode used in drug and DNA delivery *in vivo*: analytical versus numerical solution, *IEEE Trans. Biomed. Eng.* 50 (2003) 1296–1300.
- [5] J.J. Drabick, J. Glasspool-Malone, A. King, R.W. Malone, Cutaneous transfection and immune responses to intradermal nucleic acid vaccination are significantly enhanced by *in vivo* electroporation, *Mol. Ther.* 3 (2001) 249–255.
- [6] C. Faurie, M. Golzio, P. Moller, J. Teissie, M.P. Rols, Cell and animal imaging of electrically mediated gene transfer, *DNA Cell. Biol.* 22 (2003) 777–783.
- [7] C. Faurie, E. Phez, M. Golzio, C. Vossen, J.C. Lesbordes, C. Delteil, J. Teissie, M.P. Rols, Effect of electric field vectoriality on electrically mediated gene delivery in mammalian cells, *Biochim. Biophys. Acta* 1665 (2004) 92–100.
- [8] B. Gabriel, J. Teissie, Time courses of mammalian cell electroporation observed by millisecond imaging of membrane property changes during the pulse, *Biophys. J.* 76 (1999) 2158–2165.
- [9] S.A. Gallo, P.G. Johnson, S.W. Hui, Using surface electrodes to monitor the electric pulse-induced permeabilization of porcine skin, *Methods Mol. Med.* 7 (2003) 437–445.
- [10] J. Gehl, T.H. Sorensen, K. Nielsen, P. Raskmar, S.L. Nielsen, T. Skorvsgaard, L.M. Mir, *In vivo* electroporation of skeletal muscle: threshold, efficacy and relation to electric field distribution, *Biochim. Biophys. Acta* 1428 (1999) 233–240.
- [11] J. Gehl, Electroporation: theory and methods, perspectives for drug delivery, gene therapy and research, *Acta Physiol. Scand.* 177 (2003) 437–447.
- [12] M. Golzio, J. Teissie, M.P. Rols, Direct visualization at the single-cell level of electrically mediated gene delivery, *Proc. Natl. Acad. Sci. U. S. A.* 99 (2002) 1292–1297.
- [13] R.A. Gilbert, M.J. Jaroszeski, R. Heller, Novel electrode designs for electrochemotherapy, *Biochim. Biophys. Acta* 1334 (1997) 9–14.
- [14] R. Heller, Delivery of plasmid DNA using *in vivo* electroporation, *Preclinica* 1 (2003) 198–208.
- [15] R. Heller, M. Jaroszeski, A. Atkin, D. Moradpour, R. Gilbert, J. Wands, C. Nicolau, *In vivo* gene electroinjection and expression in rat liver, *FEBS Lett.* 389 (1996) 225–228.
- [16] R. Heller, J. Schultz, M.L. Lucas, M.J. Jaroszeski, L.C. Heller, R.A. Gilbert, et al., Intradermal delivery of interleukin-12 plasmid DNA by *in vivo* electroporation, *DNA Cell Biol.* 20 (2001) 21–26.
- [17] G.A. Hofmann, Instrumentation and electrodes for *in vivo* electroporation, *Methods Mol. Med.* 37 (2000) 37–62.
- [18] Z. Huang, M. Tamura, T. Sakurai, S. Chuma, T. Saito, N. Nakasutji, *In vivo* transfection of testicular germ cells and transgenesis by using the mitochondrially localized jellyfish fluorescent protein gene, *FEBS Lett.* 487 (2000) 248–251.
- [19] M.J. Jaroszeski, R.A. Gilbert, R. Heller, *In vivo* antitumor effects of electrochemotherapy in a hepatoma model, *Biochim. Biophys. Acta* 1334 (1997) 15–18.
- [20] J.M. McMahon, D.J. Wells, Electroporation for gene transfer to skeletal muscles: current status, *BioDrugs* 18 (2004) 155–165.
- [21] D. Miklavcic, K. Beravs, D. Semrov, M. Cemazar, F. Demsar, G. Sersa, The importance of electric field distribution for effective *in vivo* electroporation of tissues, *Biophys. J.* 74 (1998) 2152–2158.
- [22] D. Miklavcic, D. Semrov, H. Mekid, L.M. Mir, A validated model of *in vivo* electric field distribution in tissues for electrochemotherapy and for DNA electrotransfer for gene therapy, *Biochim. Biophys. Acta* 1523 (2000) 73–83.
- [23] L.M. Mir, L.F. Glass, G. Sersa, J. Teissie, C. Domenge, D. Miklavcic, et al., Effective treatment of cutaneous and subcutaneous malignant tumours by electrochemotherapy, *Br. J. Cancer* 77 (1998) 2336–2342.
- [24] L.M. Mir, M.F. Bureau, J. Gehl, R. Rangara, D. Rouy, J.M. Caillaud, et al., High-efficiency gene transfer into skeletal muscle mediated by electric pulses, *Proc. Natl. Acad. Sci. U. S. A.* 96 (1999) 4262–4267.
- [25] M. Pavlin, N. Pavselj, D. Miklavcic, Dependence of induced transmembrane potential on cell density, arrangement, and cell position inside a cell system, *IEEE Trans. Biomed. Eng.* 49 (2002) 605–612.
- [26] U. Pliquet, Joule heating during solid tissue electroporation, *Med. Biol. Eng. Comput.* 41 (2003) 215–219.
- [27] M. Puc, S. Corovic, K. Flisar, M. Petkovsek, J. Nastran, D. Miklavcic, Techniques of signal generation required for electroporation. Survey of electroporation devices, *Bioelectrochemistry* 64 (2004) 113–124.
- [28] M.P. Rols, J. Teissie, Electroporation of mammalian cells: quantitative analysis of the phenomenon, *Biophys. J.* 58 (1990) 1089–1098.
- [29] M.P. Rols, C. Delteil, M. Golzio, P. Dumond, S. Cros, J. Teissie, *In vivo* electrically mediated protein and gene transfer in murine melanoma, *Nat. Biotechnol.* 16 (1998) 168–171.
- [30] M.P. Rols, Y. Tamzali, J. Teissie, Electrochemotherapy of horses, a preliminary clinical report, *Bioelectrochemistry* 55 (2002) 101–106.
- [31] D. Semrov, D. Miklavcic, Calculation of the electrical parameters in electrochemotherapy of solid tumours in mice, *Comput. Biol. Med.* 28 (1998) 439–448.
- [32] D. Sel, S. Mazeres, J. Teissie, D. Miklavcic, Finite-element modeling of needle electrodes in tissue from the perspective of frequent model computation, *IEEE Trans. Biomed. Eng.* 50 (2003) 1221–1232.
- [33] G. Sersa, M. Cemazar, D. Semrov, D. Miklavcic, Changing electrode orientation improves the efficacy of electrochemotherapy of solid tumors in mice, *Bioelectrochem. Bioenerg.* 39 (1996) 61–66.
- [34] A. Titomirov, S. Sukarev, E. Kistanova, *In vivo* electroporation and stable transformation of skin cells of newborn mice by plasmid DNA, *Biochim. Biophys. Acta* 1088 (1991) 131–134.
- [35] D. Miklavcic, S. Corovic, G. Pucihar, N. Pavselj, Importance of tumour coverage by sufficiently high local electric field for effective electrochemotherapy, *Eur. J. Cancer Suppl.* 4 (2006) 45–51.
- [36] B. Valic, M. Golzio, M. Pavlin, A. Schatz, C. Faurie, B. Gabriel, J. Teissie, M.P. Rols, D. Miklavcic, Effect of electric field induced transmembrane potential on spherical cells: theory and experiment, *Eur. Biophys. J.* 32 (2003) 519–528.
- [37] L.C. Heller, M.J. Jaroszeski, D. Coppola, A.N. McCray, J. Hickey, R. Heller, Optimization of cutaneous electrically mediated plasmid DNA delivery using novel electrode, *Gene Ther.* 14 (2007) 275–280.
- [38] S.M. Kennedy, Z. Ji, J.C. Hedstrom, J.H. Booske, S.C. Hagness, Quantification of electroporative uptake kinetics and electric field heterogeneity effects in cells, *Biophys. J.* 94 (2008) 5018–5027.
- [39] B.J. Mossop, R.C. Barr, J.W. Henshaw, D.A. Zaharoff, F. Yuan, Electric fields in tumors exposed to external voltage sources: implication for electric field-mediated drug and gene delivery, *Ann. Biomed. Eng.* 34 (2006) 1564–1572.
- [40] S. Pedron-Mazoyer, J. Plouet, L. Hellaudais, J. Teissie, M. Golzio, New anti angiogenesis developments through electro-immunization: optimization by *in vivo* optical imaging of intradermal electro gene transfer, *Biochim. Biophys. Acta* 1770 (2007) 137–142.
- [41] M.N. Torrero, W.G. Henk, S. Li, Regression of high-grade malignancy in mice by bleomycin and interleukin-12 electrochemotherapy, *Clin. Cancer Res.* 12 (2006) 257–263.
- [42] T. Kishida, H. Asada, Y. Itokawa, K. Yasutomi, M. Shin-Ya, S. Gojo, F.D. Cui, Y. Ueda, H. Yamagishi, J. Imanishi, O. Mazda, Electrochemo-gene therapy of cancer: intratumoral delivery of interleukin-12 gene and bleomycin synergistically induced therapeutic immunity and suppressed subcutaneous and metastatic melanomas in mice, *Mol. Ther.* 8 (2003) 738–745.
- [43] M. Yang, E. Baranov, A.R. Moossa, S. Penman, R.M. Hoffman, Visualizing gene expression by whole-body fluorescence imaging, *Proc. Natl. Acad. Sci. U. S. A.* 97 (2000) 12278–12282.
- [44] U. Pliquet, J.C. Weaver, Feasibility of an electrode-reservoir device for transdermal drug delivery by noninvasive skin electroporation, *IEEE Trans. Biomed. Eng.* 54 (2007) 536–538.